Chemical and toxicological characterization of vaping emission products from commonly used vape juice diluents

Huanhuan Jiang [†‡], C. M. Sabbir Ahmed [§], Thomas J. Martin [‖], Alexa Canchola [§], Iain W. H. Oswald [‖], Jose An-dres Garcia [‡], Jin Y. Chen [§], Kevin A. Koby [‖], Anthony J. Buchanan [⊥], Zixu Zhao [#], Haofei Zhang [#], Kunpeng Chen [†], and Ying-Hsuan Lin [†,§]*

[†] Department of Environmental Sciences, University of California, Riverside, California 92521, United States;

[‡] Department of Chemical & Environmental Engineering, University of California, Riverside, California 92521, United States;

[§] Environmental Toxicology Graduate Program, University of California, Riverside, California 92521, United States;

[‖] Abstrax Tech, 15550 Rockfield Blvd, Suite B120, Irvine, California 92618, United States;

[⊥] SepSolve Analytical Ltd., 4 Swan Court, Forder Way, Peterborough Cambridgeshire, PE7 8GX, United Kingdom;

[#] Department of Chemistry, University of California, Riverside, California 92521, United States;

KEYWORDS. e-cigarette, liquid diluents, viscosity enhancer, chemical composition, cellular toxicity

Table of Contents

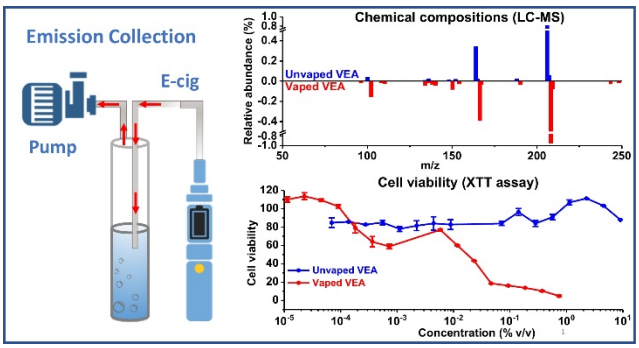

ABSTRACT

Recent reports have linked severe lung injuries and deaths to the use of e-cigarettes and vaping products. Nevertheless, the causal relationship between exposure to vaping emissions and the observed health outcomes remains to be elucidated. Through chemical and toxicological characterization of vaping emission products, this study demonstrates that during vaping processes, changes in chemical composition of several commonly used vape juice diluents (also known as cutting agents) lead to the formation of toxic byproducts, including quinones, carbonyls, esters and alkyl alcohols. The resulting vaping emission condensates cause inhibited cell proliferation and enhanced cytotoxicity in human airway epithelial cells. Notably, substantial formation of the duroquinone and durohydroquinone redox couple was observed in the vaping emissions from vitamin E acetate, which may be linked to acute oxidative stress and lung injuries reported by previous studies. These findings provide an improved molecular understanding and highlight the significant role of toxic byproducts in vaping-associated health effects.

1. INTRODUCTION

Recent outbreaks of the mysterious vaping-related illness, also known as EVALI (e-cigarette or vaping product use-associated lung injury) in users of e-cigarettes and vaping products have raised serious public health concerns.[1-3] Within a few months since its description, the disease has affected more than 2800 people (as of February 18, 2020), and resulted in an increasing number of fatal cases in the United States.[1, 2, 4] The substances responsible for the lung injury are still under investigation.[5] Though it appears that tetrahydrocannabinol (THC)-containing vaping products and vitamin E acetate found in patients' lung fluids are strongly linked to the outbreak of lung injuries,[6] the causal relationship remains unclear. Additionally, since vaping emissions constitute a complex, dynamic and reactive mixture, there may be more than one factor leading to the vaping-related lung injury.

THC-containing vaping products are generally sold either in pre-filled vape cartridges, or in dropper bottles that allow users to refill vape pen cartridges themselves. THC vape cartridges are usually cut with thickening agents, such as vitamin E acetate (VEA),[6, 7] to enhance the viscosity of THC oil and make it appear pure to consumers. Given that THC is lipophilic, it can be easily mixed with organic solvents, but not water. Thus, commonly used vape juice diluents including propylene glycol (PG), vegetable glycerin (VG), squalane oil (SQL) and coconut oil or medium-chain triglyceride (MCT) oil are suitable to dilute the THC oil. Some of these liquid diluents and viscosity enhancers are generally considered as safe additives for food via ingestion. However, their safety has not been fully assessed for vaping inhalation, a process that can potentially transform the liquid ingredients and produce reactive and toxic compounds.[8-10] It has been reported that reactive carbonyls including acrolein, formaldehyde and acetaldehyde can be emitted from the thermal decomposition of e-liquids through the heating process during vaping.[11-14] The emission

rates of aldehydes can be influenced by several factors including e-liquid composition, power supply, device model, coil material and vaping topography.[11-14]

While the chemical and toxicological properties of vaping emission products from PG and VG have been widely studied,[11, 15-18] little is known about the vaping emission products from other commonly used liquid diluents. In this study, we examined seven commonly used vape juice diluents in THC-infused e-cigarette cartridges, including PG, VG, MCT oil, SQL, vitamin E (VE), VEA and triethyl citrate (TEC) (Table 1). The chemical composition of unvaped liquid diluents and collected vaping emission condensates were analyzed by gas chromatography/electron ionization-mass spectrometry (GC/EI-MS) and electrospray ionization quadrupole-time of flight-mass spectrometry (ESI-Q-TOF-MS) techniques. BEAS-2B cells were exposed to emission samples collected in the LHC-9 cell medium. Cell viability and cytotoxicity were examined by the XTT assay to determine the metabolic activity and the LDH assay to measure of the cell membrane integrity after exposure. We hypothesize that chemical composition of vaping emission products is an important determinant of vaping-induced toxicity. Changes in chemical composition of liquid diluents through thermal decomposition or oxidation during vaping can result in differential cellular toxicity compared to their unvaped precursors.

2. METHODS.

2.1. Materials. Samples of vape liquid diluents were purchased to emulate those used in vaping as closely as possible and used as received. Triethyl citrate (TEC) was purchased from Sigma-Aldrich (>99%), Vitamin E acetate (VEA) was purchased from Whole Foods (JASON brand), Vitamin E (VE) and MCT oil were purchased from Jedwards International Inc, Propylene glycol (PG) was purchased from Spectrum Chemical (99.5%), vegetable glycerin (VG) was purchase from Spectrum Chemical (99%) , and squalane (SQL) was purchased from Jedwards International

Inc. Products were inventoried and stored at room temperature. N,O-bis(trimethylsilyl)trifluoroacetamide with trimethylchlorosilane (BSTFA + TMCS, 99:1) was purchased from SUPELCO. Anhydrous pyridine (≥99%) was purchased from EMD Millipore Corporation. Isopropyl alcohol (IPA, 99.5%) was purchased from VWR Analytical. Methanol (99.9%) and acetonitrile (ACN, 99.95%) were purchased from Fisher Scientific. O-(2,3,4,5,6-pentafluorobenzyl) hydroxylamine hydrochloride (PFBHA, ≥98%) was purchased from Sigma Aldrich.

2.2. Sample collection for chemical analysis. The vape pen (Max Battery) was connected to an authentic CCell cartridge (510 thread, 0.5 mL, TH205, 1.4 Ω) filled with individual liquid diluents and operated under 3.6 V (i.e., 9.26 watt). The cartridge is equipped with a wick that has a ceramic core with a nichrome wire to activate the core. The cartridge has a ceramic mouthpiece and transparent glass window. Before each collection, the vape pen was pre-conditioned by taking three puffs. Gases and aerosols produced from different liquid diluents were collected at room temperature in a 30 mL impinger, each containing 15 mL of isopropyl alcohol (IPA), acetonitrile (ACN), or o-(2,3,4,5,6-pentafluorobenzyl)hydroxylamine hydrochloride (PFBHA) aqueous solution (4 mg/mL). One puff was 4 s followed by 60 s rest time to avoid overheating the pen. Total 10 puffs were collected for chemical analysis. The flow rate was controlled by a 0.18 lpm critical orifice connected to a mini diaphragm pump (YW02-DC24, Changzhou Yuanwang Technology). The chemical composition of unvaped liquid diluents and collected vaping emission condensates were analyzed by GC/EI-MS and ESI-Q-TOF-MS. Samples collected in IPA and ACN were directly injected to GC/EI-MS and Q-TOF-MS, respectively. A fraction of vaping emission samples collected in ACN were derivatized with N,O-bis(trimethylsilyl)trifluoroacetamide (BSTFA) prior to GC/EI-MS analysis to identify products

containing hydroxyl functional groups.[19] Samples collected in aqueous PFBHA solutions were extracted by hexane before GC/EI-MS analysis to identify carbonyl-containing compound.[20] Details of derivatization and GC/EI-MS analysis are given in the Sections 2.4-2.6. To determine the collection efficiency of the impinger, two impingers were connected in tandem to determine the breakthrough of samples. 10 μL 4-fluorobenzaldehyde (2 μg/μL) was added as an internal standard to each impinger before collection. Note that 4-fluorobenzaldhyde can be detected directly by GC/EI-MS without derivatization with fragments of *m*/*z* 51, 75, 95, 123, and 124. The overall collection efficiency of impinger was estimated to be 98.9%-100% by comparing the normalized peak areas of several target analytes in the front and back impinger samples (Table S1). Peak areas of impingers samples were normalized by that of 4-fluorobenzaldehyde. The aerosol collection efficiency was determined to be ~80% by comparing the particle size and volume distribution in the inflow and outflow of the impinger collection system (Figure S1).

2.3. Sample collection for cell exposure. Before each collection, the vape pen was preconditioned by taking three puffs. For the cell viability and cytotoxicity assays, 100 puffs of vaping emissions were collected into an impinger filled with 15 mL of LHC-9 media (Gibco, Invitrogen). The total consumption of liquid diluents for 100 puffs were shown in Table 1.

2.4. BSTFA derivatization. 50-100 μL of impinger samples collected with ACN were reacted with 50 μL BSTFA and 50 μL pyridine at 70 °C for one hour. The reaction mixtures were subsequently analyzed by GC/EI-MS.

2.5. PFBHA derivatization. The PFBHA derivatization procedures were modified from those published by Yu et al.[20] As mentioned earlier, 4-fluorobenzadehyde (10 μL of 2 μg/μL solution) was added as an internal standard to the impinger before the sample collection. The samples were allowed to react with PFBHA for 24 h before the addition of 0.3 mL 6N HCl. Then, 3 mL of

hexane was added to extract the pentfluorobenzyl oxime derivatives from reaction of carbonyls with PFBHA, followed by the addition of about 50 mg of Na_2SO_4 to remove water. Then, samples were transferred to GC vials and analyzed by GC/EI-MS.

2.6. GC/EI-MS analysis. The detailed procedures for GC/EI-MS analysis have been reported in our previous studies.[21] The impinger samples were analyzed by an Agilent 6890N GC coupled with 5975 MSD using electron ionization (EI) technique. 5 μL of each sample was programmed to be injected to a separation column (J&W Scientific DB-5, 30 m × 0.25 mm i.d., 0.25 μm film). The same GC temperature profile was used for both PCI and EI analysis. The temperature of GC was set at 60 °C for 1 min, ramped up to 200 °C with a rate of 3 °C min^{-1}, held at 200 °C for 2 min, ramped up to 310 °C with a rate of 20 °C min^{-1}, and finally held at 310 C for 10 min. The solvent delay time was tuned for different solvent, i.e., 10.5 min for samples containing BSTFA and 4 min for other solvents. Compound identification was performed using the NIST 2014 mass spectral database. Compounds with a matching rate larger than 40% were reported in Table S2-8.

For VE and VEA samples, three replicates were conducted for each diluent. Also, 10 μL of 1 μg/ μL acenaphthene-d10 was added as an internal standard to each sample before collection. The concentrations of duroquinone and durohydroquinone were calibrated using corresponding standards. Note that both duroquinone and durohydroquinone can be detected by GC/EI-MS without derivatization, but GC/EI-MS has much higher sensitivity for duroquinone than durohydroquinone. As shown in Figure S2, duroquinone was identified with EI fragment of m/z 54, 93, 121, 136, and 164. Durohydroquinone was identified with fragments of m/z 123, 151, and 166.

2.7. ESI-Q-TOF-MS analysis. Impinger samples collected with ACN were directly introduced to the quadruple-time of flight-mass spectrometer (Q-TOF-MS, Agilent 6545) using a syringe pump.

The flow rate of the syringe pump was 0.2 mL/min. The obtained data files were analyzed using the Agilent MassHunter Qualitative Analysis software. Compounds with relative abundance >5% and measured *m/z* difference from theoretical *m/z* < 2 mDa from were reported in Table S9-15.

2.8. Cell culture. Human bronchial epithelial cells (BEAS-2B) were obtained from the American Type Culture Collection (ATCC). The BEAS-2B cell line was derived from normal bronchial epithelium obtained from autopsy of non-cancerous individuals and immortalized using a replication-defective SV40/adenovirus 12 hybrid.[22] Cells were cultured in LHC-9 medium and grown at 37°C and 5% CO_2 in a humidified incubator. Cells were cultured in T-75 flasks at a density of 3×10^5 cells/flask. The cell medium was replaced every other day. Upon 80-90% confluency, cells were harvested using phosphate-buffered saline (PBS) for washing and incubated with 4 mL of 0.25% trypsin EDTA/PBS for 3 min at 37 °C to allow detachment. Cells were seeded in 96-well plates at a density of 5×10^3 cells per well in 100 μL of LHC-9 medium for 24 hours prior to exposure. At the time of exposure, cells reached a 60−70% confluency. Cells were washed with PBS and then exposed to unvaped liquid diluents and vaping emission samples for 48 hours.[22, 23] The stock solution of unvaped oil solutions were prepared directly in LHC-9 medium. For SQL, VE, VEA and MCT, 1% v/v DMSO was added to the stock solution increase the solubility. The stock solutions were then diluted using LHC-9 medium into 18 different concentrations with 2-fold dilution. The vaping emission samples collected by the impinger were also diluted into 18 different concentrations before applied to the cell exposure. Cells exposed to only media were included as negative controls. 1% v/v DMSO was used as the vehicle control and no significant cytotoxicity was observed.

2.9. Cell Viability (XTT) and Cytotoxicity (LDH) Assays. The cellular toxicity of unvaped liquid diluents and their vaping emissions was determined using 3-bis-(2-methoxy-4-nitro-5-

sulphenyl)-(2H)-tetrazolium-5-carboxanilide (XTT) and lactate dehydrogenase (LDH) assays. Treatments were performed with serial two-fold dilutions in 96-well plates. Unexposed cells were included as negative controls. The highest concentration contained 10 μL-consumed oil/μL-cell media for unvaped liquid diluents and 100 puffs/15 mL solutions of collected the vaping emission samples (Table 1). Cells were exposed for 48 h before the XTT and LDH assays were performed. The XTT assay is based on the conversion of the water-soluble XTT reagent to an orange formazan product by metabolically active cells. The fluorometric LDH assay was performed to assess the cell membrane integrity and cytotoxicity of cells, following the CytoTox-ONE™ homogeneous membrane integrity assay protocol (Promega). Triton X-100 (0.1%) was used as a positive control to simulate 100% cell death. The absorbance for XTT assay was measured using a TECAN SpectraFluor Plus microplate reader at 490 nm, with a reference wavelength at 620 nm. The fluorescence for LDH assay (excitation 560/emission 590 nm) was also measured with the same plate reader.

3. RESULTS AND DISCUSSIONS.

Overall, the results revealed significant changes in chemical composition and a shift of cellular toxicity in cells exposed to vaping emission condensates compared to the unvaped liquid diluents, supporting our hypothesis that toxic byproducts formed during the vaping process are important to induce vaping-associated health effects. Combining information from Figure 1, Table S2-8 (GC/EI-MS) and Table S9-15 (ESI-Q-TOF-MS), the chemical compositions of vaping emission products are very different from their parent liquid diluents, showing formation of new products in vaping emissions. The detected new products include carbonyls, alkyl alcohols, esters, carboxylic acids and short chain alkanes, likely resulting from thermal decomposition and oxidation of liquid diluents. Along with changes in chemical composition, a large decrease of cell

viability measured by the XTT assay was observed for most vaping emissions compared to unvaped liquid diluents (Figure 2A), except for TEC that showed similar cellular response to both vaping emissions and its unvaped precursor. An increase of LDH release that acts as an indicator of damaged cell membrane integrity was observed for cells exposed to MCT, SQL, and VE vaping emission products.

3.1. PG and VG. The chemical compositions of PG and VG oil changed significantly after vaping. We observed a series of oligomers in unvaped PG oil but only $C_6H_{14}O_3$ in its vaping emissions (Figure 1). A dimer $C_6H_{12}O_4$ was detected in both unvaped and vaped VG. Oligomers were also reported in particles emitted from PG and VG vaping previously by Escobar et al.[24] Various carbonyls were generated from the vaping emissions of PG, including acetaldehyde, acetone, propionaldehyde, 1,3-dihydroxypropanone, and 2-oxopropanal (Table S2). Seven different carbonyls were detected from vaping emissions of VG, including formaldehyde, acetaldehyde, acetone, 1,2-dihydroxypropanone, oxalaldehyde, 2-oxopropanal, and pentane-2,4-dione (Table S3). The production of carbonyls from the vaping of PG and VG may contribute to the increased cellular toxicity (i.e., left-shift in the concentration-response curve) as measured by the XTT assay (Figure 2A). Note that VG has higher viscosity, which causes thicker cloud production during vaping.[18] The fluid starvation in the wick may lead to the "dry puff" conditions (i.e., overheating of the coil) and result in increased production of carbonyls.[8] Thus, the vaping emission products from neat (100%) VG may not represent the vaping scenarios when blends of PG and VG mixture are used as vaping liquids.

3.2. MCT oil and SQL. For MCT oil that contains mostly glycerol tricaprylate, dinonaoin monocaprylin, and 1,2,3-propanetriyl ester decanoic acid, and SQL that has a long alkyl chain (not detectable in Figure 1 because it cannot be ionized efficiently within the ESI), these unvaped oils

did not induce obvious loss of cell viability or lead to damaged cell membrane integrity. However, the liquid diluents transformed substantially after vaping. Short chains esters (e.g., n-octanoic acid isopropyl ester, methyl ester decanoic acid, and i-propyl decanoate) and short chains alkanes (e.g., e-theyl-octane, 2,6,10- trimethyl-dodecane and 2,6,10,15-tetramethyl heptadecane) were produced from the vaping of MCT oil (Table S4) and SQL (Table S5), respectively. Also, short chain carbonyls were found in both MCT (e.g., formaldehyde, 2-butanone, 2-pentanone, and n-heptanal) and SQL (e.g., 3-methylpentanal and n-nonanal) vaping emissions. Notably, alkyl alcohols were also observed, 2-tridecan-1-ol in vaping emissions of MCT oil and 6,10,14-trimethyl-pentadecan-2-ol in vaping emissions of SQL. These alcohols are surfactant-like, with a nonpolar hydrophobic tail (i.e., the alkyl group) and a polar hydrophilic head (i.e., the hydroxyl group). It has been reported that alkyl alcohols can elicit a number of cellular responses that are potentially cytotoxic and can affect membrane structure and compromise cell function.[25] The production of oxygenated products (e.g., esters and carbonyls) from vaping of MCT oil and SQL may contribute to the observed decrease in cell viability compared to the parent compounds (Figure 2A). The production of alkyl alcohols in vaping emissions of MCT oil and SQL may explain the elevated LDH release shown in Figure 2B when cells were exposed to vaping emission samples with concentrations $\geq 6.9\times10^{-2}$ % v/v for SQL and $\geq 2.8\times10^{-4}$ % v/v for MCT oil vaping emission samples, respectively.

3.3. VE and VEA. Unvaped VE and VEA also did not show notable cell death. However, a sharp decrease in cell viability was seen after vaping (Figure 2A). We detected oligomers in unvaped VE oil (Figure 1) but not in the VE vaping emission samples. Degradation and oxidation compounds such as acetone and 3,7,11-trimethyl-1-dodecanol were observed in vaping emissions from VE and VEA. It has been reported that exposure to acetone can lead to irritation to respiratory tract and oxidative stress.[26] As a long chain alcohol, 3,7,11-trimethyl-1-dodecanol could increase

246 cell membrane permeability and cytotoxicity of vaping emissions, which may explain the slight
247 increase of LDH release from cells exposed to vaping samples (Figure 2B).

248 Most importantly, we observed quinone-like compounds from the vaping of VE and VEA
249 (Figure 3, Table S6-7, and Figure S2), with 0.89±0.09 μg/mg-diluent of duroquinone (DQ) from
250 VE vaping, and 2.45±0.23 μg/mg-diluent of DQ and 12.00±1.10 μg/mg-diluent of
251 durohydroquinone (DHQ) from VEA vaping. Since quinone-like compounds are significant
252 contributors to the generation of reactive oxygen species through redox reaction,[27] they might
253 explain the significant increase of cytotoxicity of VE and VEA vaping samples, acute oxidative
254 stress and the reported EVALI cases.[3, 6, 7] The presence of DQ and DHQ has been reported in
255 previous studies,[28, 29] but as far as we know, this is the first study to quantify the yield of DQ and
256 DHQ from vaping of VE and VEA. Future studies are warranted to further investigate the role of
257 DQ and DHQ redox couple in cellular oxidative stress and EVALI.

258 **3.4. TEC.** For TEC, we observed decomposition of the parent compound. Smaller esters were
259 detected in the vaping emissions of TEC, including diethyl ester propanedioic acid, malonic acid
260 diisopropyl ester, diethyl ester propanedioic acid, and o-acetylcitric acid triethyl ester. (Table S8)
261 These products might be formed from thermal degradation of TEC. Notably, both unvaped TEC
262 and its vaping emissions showed decreased cell viability in a concentration-dependent manner,
263 while no significant LDH release (damage to cell membrane integrity) was found for cells exposed
264 to this liquid diluent (Figure 2 A-B). We also observe a decrease of cell viability for TEC vaping
265 samples compared to unvaped TEC, but the difference was not as significant as other oils.

266 **3.5. Potential limitations.** While the study provides an improve molecular understanding
267 regarding chemical composition change after vaping and cellular toxicity, cautions should be taken
268 when interpreting these results in real-world vaping conditions. (1) The vaping topography applied

in the current study was not intended to mimic the real vaping scenarios, but rather to ensure high collection efficiency of vaping emissions in impinger samples. This study applied a small puff volume (12 ml) and a low puff frequency (1 puff/min).The puff patterns may change the chemical composition of vaping emissions.[12, 30, 31] According to the study by Beauval et al.,[12] among 6 measured aldehydes (formaldehyde, acrolein, acetaldehyde, propionaldehyde, acetone, and methylglyoxal), the production of acrolein (ng-aldehyde/mg-consumed e-liquid) showed a significant decrease with a decreased puff volume, and the generation of all these aldehydes showed either a slight decrease or no significant change with the decrease of puff frequency. Thus, a more realistic puff pattern should be considered for future studies to provide a more representative profile of the vaping emission products. (2) In this study, the liquid diluents were studied individually in an isolated system to examine the formation of new compounds from the precursor. However, vaping liquids often contain various ratios of blends (e.g., PG/VG) and also mixed with flavoring compounds. The emissions products from a mixture of various precursor compounds will further increase the complexity when interpreting the chemical and toxicological properties of vaping emissions. For example, Conklin et al. reported that with the increased of VG or the decrease of PG/VG ratio, formaldehyde and acrolein in aerosols increased but acetaldehyde in aerosols decreased.[32] The study by Khlystov et al. reported that the flavoring compounds in e-liquids dominated the production of aldehydes.[10] Therefore, in future studies the mixture effects of diluents and flavoring compounds in e-liquids need to be considered when comparing the chemical and toxicological properties of unvaped e-liquid and vaped emissions. (3) The current study only examined the acute cytotoxic effects of vaping emissions from commonly used liquid diluents. The chronic effects of vaping and detailed toxicity mechanisms require further investigations. (4) The emission samples collected by the impinger method included both gas and

aerosol phase products. The collection efficiency of impinger was only 80% for aerosols. Given the high proportion of particulate toxic compounds reported by recent research,[33] further studies are warranted to optimize the sample collection method for aerosol phase vaping products to more accurately estimate the exposure-induced health effects.

4. CONCLUSION.

In summary, this study provides evidence that changes in chemical composition of liquid diluents during vaping may modulate the cellular toxicity in human airway epithelial cells. In particular, formation of the thermally transformed toxic byproducts (e.g., carbonyls, esters, alkyl alcohols and quiones), many of which are known toxicants and carcinogens, is quite concerning.[34, 35] Given that the mechanistic understanding of vaping-related illness is still incomplete, these findings highlight the urgent need to further understand the underlying molecular basis of EVALI. More extensive research is warranted to evaluate sublethal toxicological endpoints to provide better insights into vaping-induced long-term health effects.

ASSOCIATED CONTENT

Supporting Information.

The data used to calculate impinger collection efficiency (Table S1); The identified vaping emission products from liquid diluents using GC/EI-MS analysis (Table S2-S8); The identified vaping products (with relative abundance larger than 5%) from liquid diluents using ESI-Q-TOF-MS analysis (Table 9-15); The particle size and volume distribution in the mainstream before and after the tandem impinger collection (Figure S1); The experimental and NIST library spectrum of duroquinone and durohydroquinone (Figure S2).

ACKNOWLEDGMENTS

Huanhuan Jiang is supported by the University of California, Riverside (UCR) Chancellor's Postdoctoral Fellowship. Ying-Hsuan Lin gratefully acknowledges support from the UCR Faculty Development Award for this research. We would like to thank Dr. Jie Zhou from UCR Department of Chemistry for his assistance with the Q-TOF-MS analyses supported by NSF CHE-1828782.

ABBREVIATIONS

PFBHA: o-(2,3,4,5,6-pentafluorobenzyl)hydroxylamine hy-drochloride; BSTFA: N,O-bis(trimethylsilyl)trifluoroacetamide; PG: propylene alcohol; VG: vegetable glycerin; MCT: medium-chain triglyceride oil; SQL: squalene; TEC: triethyl citrate; VE: vitamin E; VEA: vitamin E acetate.

References.

(1) Benowitz, N. L. (2020) Seizures After Vaping Nicotine in Youth: A Canary or a Red Herring? *J. Adolesc. Health 66*, 1-2.

(2) (2020) Outbreak of Lung Injury Associated with the Use of E-Cigarette, or Vaping, Products, In *MMWR Morb Mortal Wkly Rep*, Centers for Disease Control and Prevention.

(3) King, B. A., Jones, C. M., Baldwin, G. T., and Briss, P. A. (2020) The EVALI and Youth Vaping Epidemics — Implications for Public Health. *N. Engl. J. Med. 382*, 689-691.

(4) Davidson, K., Brancato, A., Heetderks, P., Mansour, W., Matheis, E., Nario, M., Rajagopalan, S., Underhill, B., Wininger, J., and Fox, D. (2019) Outbreak of Electronic-Cigarette-Associated Acute Lipoid Pneumonia - North Carolina, July-August 2019. *MMWR Morb Mortal Wkly Rep 68*, 784-786.

(5) Lewis, N., McCaffrey, K., Sage, K., Cheng, C.-J., Green, J., Goldstein, L., Campbell, H., Ferrell, D., Malan, N., LaCross, N., Maldonado, A., Board, A., Hanchey, A., Harris, D., Callahan, S., Aberegg, S., Risk, I., Willardson, S., Carter, A., Nakashima, A., Duncan, J., Burnett, C., Atkinson-Dunn, R., and Dunn, A. (2019) E-Cigarette Use, or Vaping, Practices and Characteristics Among Persons with Associated Lung Injury - Utah, April-October 2019. *MMWR Morb Mortal Wkly Rep 68*, 953-956.

(6) Blount, B. C., Karwowski, M. P., Shields, P. G., Morel-Espinosa, M., Valentin-Blasini, L., Gardner, M., Braselton, M., Brosius, C. R., Caron, K. T., Chambers, D., Corstvet, J., Cowan, E., De Jesús, V. R., Espinosa, P., Fernandez, C., Holder, C., Kuklenyik, Z., Kusovschi, J. D., Newman, C., Reis, G. B., Rees, J., Reese, C., Silva, L., Seyler, T., Song, M.-A., Sosnoff, C., Spitzer, C. R., Tevis, D., Wang, L., Watson, C., Wewers, M. D., Xia, B., Heitkemper, D. T., Ghinai, I., Layden, J., Briss, P., King, B. A., Delaney, L.

J., Jones, C. M., Baldwin, G. T., Patel, A., Meaney-Delman, D., Rose, D., Krishnasamy, V., Barr, J. R., Thomas, J., and Pirkle, J. L. (2020) Vitamin E Acetate in Bronchoalveolar-Lavage Fluid Associated with EVALI. *N. Engl. J. Med. 382*, 697-705.

(7) Christiani, D. C. (2020) Vaping-Induced Acute Lung Injury. *N. Engl. J. Med. 382*, 960-962.

(8) Farsalinos, K. E., Voudris, V., and Poulas, K. (2015) E-Cigarettes Generate High Levels of Aldehydes Only in 'Dry Puff' Conditions. *Addiction 110*, 1352-1356.

(9) Samburova, V., Bhattarai, C., Strickland, M., Darrow, L., Angermann, J., Son, Y., and Khlystov, A. (2018) Aldehydes in Exhaled Breath during E-Cigarette Vaping: Pilot Study Results. *Toxics 6*, 46.

(10) Khlystov, A., and Samburova, V. (2016) Flavoring Compounds Dominate Toxic Aldehyde Production during E-Cigarette Vaping. *Environ. Sci. Technol. 50*, 13080-13085.

(11) Qu, Y., Szulejko, J. E., Kim, K.-H., and Jo, S.-H. (2019) The Effect of Varying Battery Voltage Output on the Emission Rate of Carbonyls Released from E-Cigarette Smoke. *Microchem. J. 145*, 47-54.

(12) Beauval, N., Verrièle, M., Garat, A., Fronval, I., Dusautoir, R., Anthérieu, S., Garçon, G., Lo-Guidice, J.-M., Allorge, D., and Locoge, N. (2019) Influence of Puffing Conditions on the Carbonyl Composition of E-Cigarette Aerosols. *Int. J. Hyg. Envir. Heal. 222*, 136-146.

(13) Son, Y., Wackowski, O., Weisel, C., Schwander, S., Mainelis, G., Delnevo, C., and Meng, Q. (2018) Evaluation of E-Vapor Nicotine and Nicotyrine Concentrations under

Various E-Liquid Compositions, Device Settings, and Vaping Topographies. *Chem. Res. Toxicol. 31*, 861-868.

(14) Saliba, N. A., El Hellani, A., Honein, E., Salman, R., Talih, S., Zeaiter, J., and Shihadeh, A. (2018) Surface Chemistry of Electronic Cigarette Electrical Heating Coils: Effects of Metal Type on Propylene glycol Thermal Decomposition. *J. Anal. Appl. Pyrolysis. 134*, 520-525.

(15) Clapp, P. W., and Jaspers, I. (2017) Electronic Cigarettes: Their Constituents and Potential Links to Asthma. *Curr. Allergy Asthm. R. 17*, 79.

(16) Lerner, C. A., Sundar, I. K., Yao, H., Gerloff, J., Ossip, D. J., McIntosh, S., Robinson, R., and Rahman, I. (2015) Vapors Produced by Electronic Cigarettes and E-Juices with Flavorings Induce Toxicity, Oxidative Stress, and Inflammatory Response in Lung Epithelial Cells and in Mouse Lung. *PLOS ONE 10*, e0116732.

(17) Orellana-Barrios, M. A., Payne, D., Mulkey, Z., and Nugent, K. (2015) Electronic Cigarettes—A Narrative Review for Clinicians. *Am. J. Med. 128*, 674-681.

(18) Li, Q., Zhan, Y., Wang, L., Leischow, S. J., and Zeng, D. D. (2016) Analysis of Symptoms and Their Potential Associations with E-liquids' Components: A Social Media Study. *BMC Public Health 16*, 674.

(19) Jiang, H., Frie, A. L., Lavi, A., Chen, J. Y., Zhang, H., Bahreini, R., and Lin, Y.-H. (2019) Brown Carbon Formation from Nighttime Chemistry of Unsaturated Heterocyclic Volatile Organic Compounds. *Environ. Sci. Technol. Lett. 6*, 184-190.

(20) Yu, J., Jeffries, H. E., and Le Lacheur, R. M. (1995) Identifying Airborne Carbonyl Compounds in Isoprene Atmospheric Photooxidation Products by Their PFBHA Oximes

Using Gas Chromatography/Ion Trap Mass Spectrometry. *Environ. Sci. Technol. 29*, 1923-1932.

(21) Chen, J. Y., Jiang, H., Chen, S. J., Cullen, C., Ahmed, C. M. S., and Lin, Y.-H. (2019) Characterization of Electrophilicity and Oxidative Potential of Atmospheric Carbonyls. *Environ. Sci. Processes Impacts 21*, 856-866.

(22) Reddel, R. R., Ke, Y., Gerwin, B. I., McMenamin, M. G., Lechner, J. F., Su, R. T., Brash, D. E., Park, J.-B., Rhim, J. S., and Harris, C. C. (1988) Transformation of Human Bronchial Epithelial Cells by Infection with SV40 or Adenovirus-12 SV40 Hybrid Virus, or Transfection via Strontium Phosphate Coprecipitation with a Plasmid Containing SV40 Early Region Genes. *Cancer Res. 48*, 1904-1909.

(23) Ahmed, C. M. S., Yang, J., Chen, J. Y., Jiang, H., Cullen, C., Karavalakis, G., and Lin, Y.-H. (2020) Toxicological Responses in Human Airway Epithelial Cells (BEAS-2B) Exposed to Particulate Matter Emissions from Gasoline Fuels with Varying Aromatic and Ethanol Levels. *Sci. Total Environ. 706*, 135732.

(24) Escobar, Y.-N. H., Nipp, G., Cui, T., Petters, S. S., Surratt, J. D., and Jaspers, I. (2020) In Vitro Toxicity and Chemical Characterization of Aerosol Derived from Electronic Cigarette Humectants Using a Newly Developed Exposure System. *Chem. Res. Toxicol.*

(25) Baker, R. C., and Kramer, R. E. (1999) Cytotoxicity of Short-Chain Alcohols. *Annu. Rev. Pharmacol. Toxicol. 39*, 127-150.

(26) Dalton, P., Wysocki, C. J., Brody, M. J., and Lawley, H. J. (1997) Perceived Odor, Irritation, and Health Symptoms Following Short-term Exposure to Acetone. *Am. J. Ind. Med. 31*, 558-569.

(27) Linhartova, P., Gazo, I., Shaliutina, A., and Hulak, M. (2013) The In Vitro Effect of Duroquinone on Functional Competence, Genomic Integrity, and Oxidative Stress Indices of Sterlet (Acipenser Ruthenus) Spermatozoa. *Toxicol. in Vitro 27*, 1612-1619.

(28) Duffy, B., Li, L., Lu, S., Durocher, L., Dittmar, M., Delaney-Baldwin, E., Panawennage, D., LeMaster, D., Navarette, K., and Spink, D. (2020) Analysis of Cannabinoid-Containing Fluids in Illicit Vaping Cartridges Recovered from Pulmonary Injury Patients: Identification of Vitamin E Acetate as a Major Diluent. *Toxics 8*, 8.

(29) Wu, D., and O'Shea, D. F. (2020) Potential for Release of Pulmonary Toxic Ketene from Vaping Pyrolysis of Vitamin E Acetate. *Proc. Natl. Acad. Sci. 117*, 6349-6355.

(30) Zhao, J., Nelson, J., Dada, O., Pyrgiotakis, G., Kavouras, I. G., and Demokritou, P. (2018) Assessing Electronic Cigarette Emissions: Linking Physico-chemical Properties to Product Brand, E-liquid Flavoring Additives, Operational Voltage and User Puffing Patterns. *Inhal. Toxicol. 30*, 78-88.

(31) McClure, E. A., Stitzer, M. L., and Vandrey, R. (2012) Characterizing Smoking Topography of Cannabis in Heavy Users. *Psychopharmacology 220*, 309-318.

(32) Conklin, D. J., Ogunwale, M. A., Chen, Y., Theis, W. S., Nantz, M. H., Fu, X.-A., Chen, L.-C., Riggs, D. W., Lorkiewicz, P., Bhatnagar, A., and Srivastava, S. (2018) Electronic cigarette-generated aldehydes: The contribution of e-liquid components to their formation and the use of urinary aldehyde metabolites as biomarkers of exposure. *Aerosol Sci Technol 52*, 1219-1232.

(33) Uchiyama, S., Noguchi, M., Sato, A., Ishitsuka, M., Inaba, Y., and Kunugita, N. (2020) Determination of Thermal Decomposition Products Generated from E-Cigarettes. *Chemi. Res. Toxicol. 33*, 576-583.

(34) Feron, V. J., Til, H. P., de Vrijer, F., Woutersen, R. A., Cassee, F. R., and van Bladeren, P. J. (1991) Aldehydes: Occurrence, Carcinogenic Potential, Mechanism of Action and Risk Assessment. *Mutat. Res. Genet. Toxicol. 259*, 363-385.

(35) Grafström, R. C. (1990) In Vitro Studies of Aldehyde Effects Related to Human Respiratory Carcinogenesis. *Mutat. Res. Rev. Genet. Toxicol. 238*, 175-184.

444 **Table 1.** Details of vaped sample collection for cell exposure
445

Oil	Structure	Puff numbers	Total volume of oil consumed (μL)	The highest equivalent concentration of liquid diluents in cell media (μL-consumed oil/μL-media)
PG		100	346	2.3 %
VG	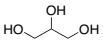	100	146	1.0 %
MCT *	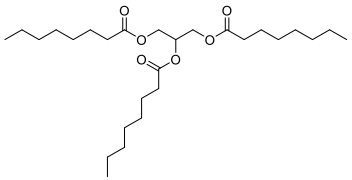	100	88	0.6 %
SQL	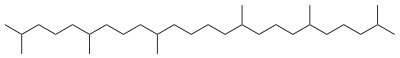	100	169	1.1 %
VE	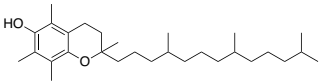	100	179	1.2 %
VEA	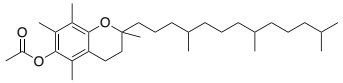	100	113	0.7 %
TEC	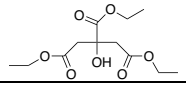	100	282	1.8 %

446 * One of three major compounds present in the mixture of MCT oil. Detailed information can be found in Table S4.

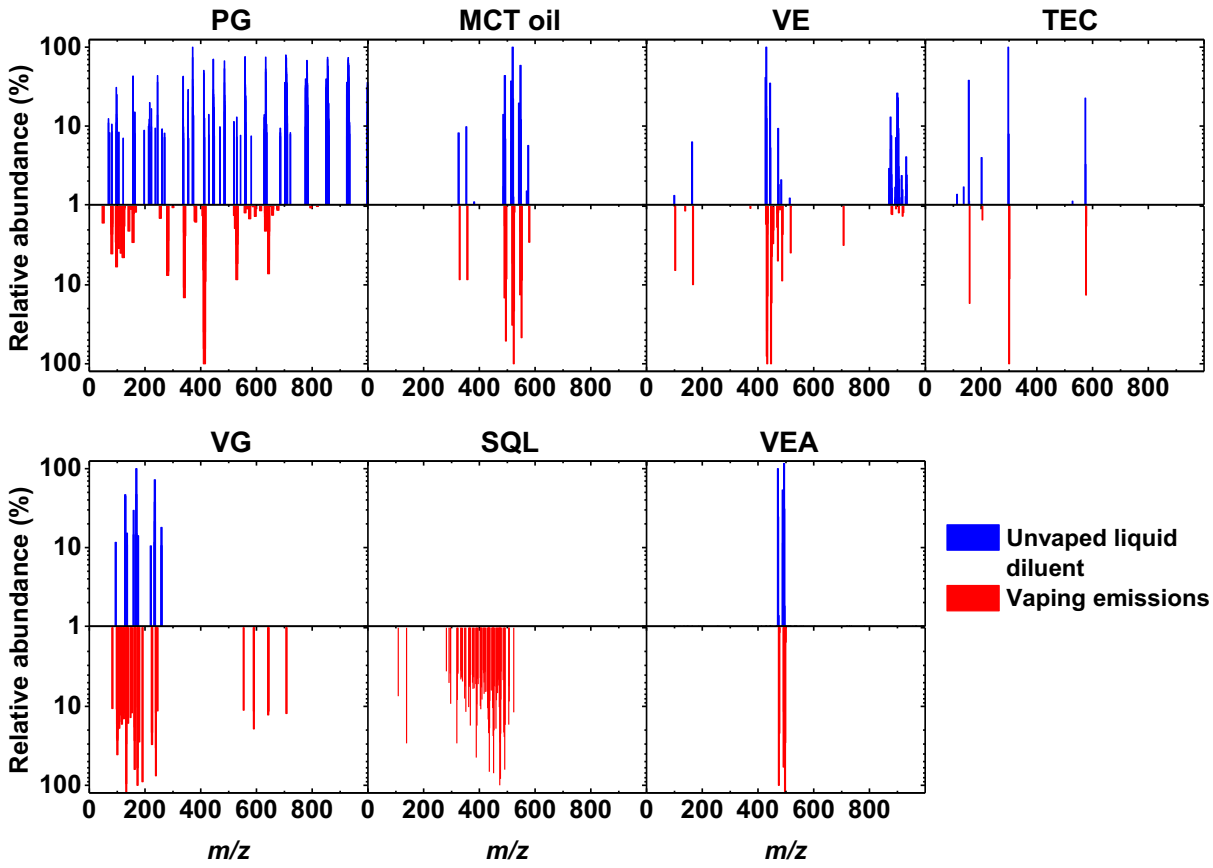

447

448 **Figure 1.** The comparative mass spectra of unvaped liquid diluents and vaping emissions
449 measured by ESI-Q-TOF-MS positive ion mode. The relative abundance was normalized to the
450 base peak of each sample. No obvious peaks were detected in the unvaped SQL sample.

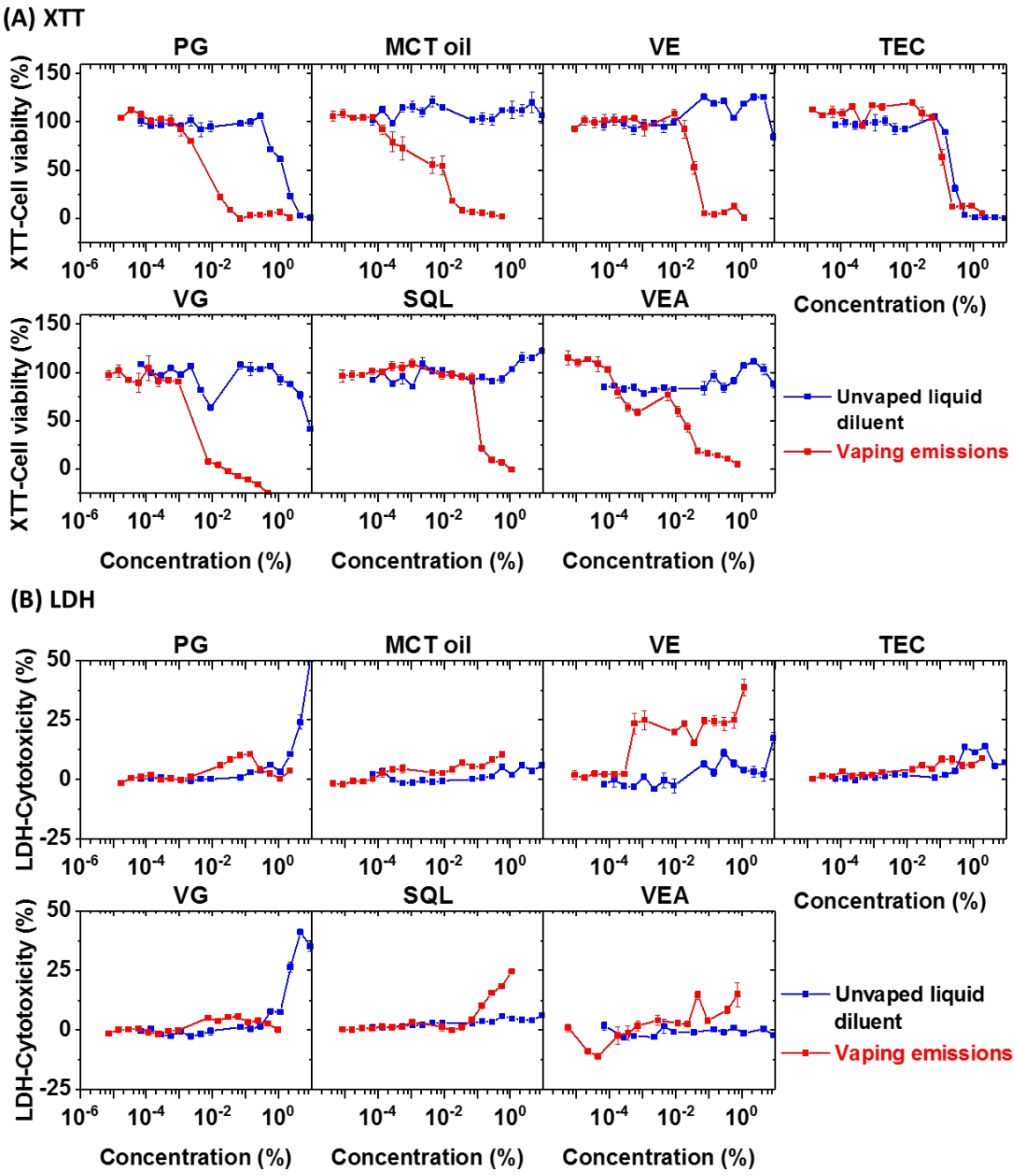

Figure 2. Cell viability and cytotoxicity curves for BEAS-2B cells treated with unvaped liquid diluents and viscosity enhancers and vaping emissions measured with (A) XTT assay and (B) LDH assay. The y axis shows the cell viability as a percentage of the untreated control (negative control). Each point is denoted as the mean ± standard error of the mean (SEM) from triplicate measurements.

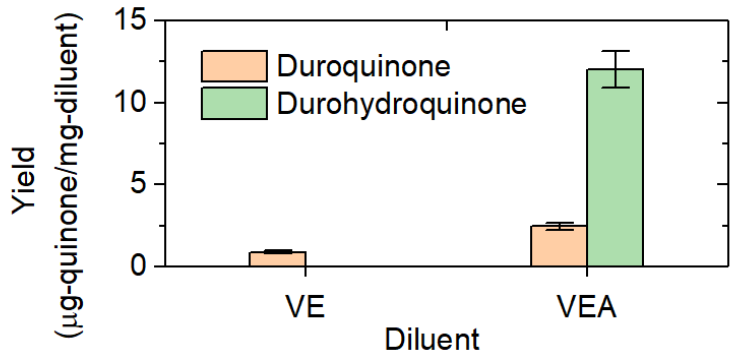

457

458 **Figure 3.** The production of duroquinone and durohydroquinone from the vaping of vitamin E and

459 vitamin E acetate. The consumption of oil (mg) is the total mass decrease of cartridge after vaping.

460 The error bar is the standard error of the mean (SEM) from measurements in triplicate.

Supporting Information

Chemical and toxicological characterization of vaping emission products from commonly used vape juice diluents

Huanhuan Jiang [†‡], C. M. Sabbir Ahmed [§], Thomas J. Martin [‖], Alexa Canchola [§], Iain W. H. Oswald [‖], Jose Andres Garcia [‡], Jin Y. Chen [§], Kevin A. Koby [‖], Anthony J. Buchanan [⊥], Zixu Zhao [#], Haofei Zhang [#], Kunpeng Chen [†], and Ying-Hsuan Lin [†§*]

[†] Department of Environmental Sciences, University of California, Riverside, California 92521, United States

[‡] Department of Chemical & Environmental Engineering, University of California, Riverside, California 92521, United States

[§] Environmental Toxicology Graduate Program, University of California, Riverside, California 92521, United States

[‖] Abstrax Tech, 15550 Rockfield Blvd, Suite B120, Irvine, California 92618, United States

[⊥] SepSolve Analytical Ltd., 4 Swan Court, Forder Way, Peterborough Cambridgeshire, PE7 8GX, United Kingdom

[#] Department of Chemistry, University of California, Riverside, California 92521, United States

* Phone: +1-951-827-3785, Email: ying-hsuan.lin@ucr.edu

Number of pages: 19

Number of tables: 15

Number of figures: 2

Table S1. The peak areas of selected compounds normalized to the peak area of 4-fluorobenzaldehyde (as an internal standard) in the front and back impingers.

	Selected *m/z* for EIC*	Front impinger	Back impinger	Collection efficiency
Duroquinone	121	1.7	Below detection limit	100%
Diethyl ester propanedioic acid	133	19.2	Below detection limit	100%
Vitamin E	430	476.5	2.5	99.5%
Formaldehyde	181	722.0	7.7	98.9%

*EIC: extracted ion chromatogram

Note: The *m*/*z*=123 (without derivatization) or 319 (with PFBHA derivatization) was selected to determine the peak area of 4-fluorobenzaldehyde.

Table S2. Identified vaping emission products from PG using GC/EI-MS analysis

Liquid Diluent	Carbonyls	Products with hydroxyl groups
Propylene glycol 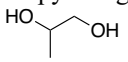	Acetaldehyde  Acetone  Propionaldehyde  1,3-Dihyroxypropanone 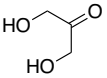 2-oxopropanal 	Propanoid acid 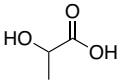

Table S3. Identified vaping emission products from VG using GC/EI-MS analysis

Liquid Diluent	Carbonyls	Products with hydroxyl groups
Vegetable glycerin 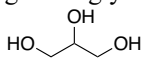	Formaldehyde  Acetaldehyde  Acetone  1,3-Dihyroxypropanone 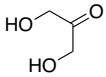 oxalaldehyde  2-oxopropanal  pentane-2,4-dione 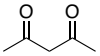	Not detectable except the parent compound.

Table S4. Identified vaping emission products from MCT oil using GC/EI-MS analysis

Liquid Diluent	Esters	Carbonyls	Products with hydroxyl groups
MCT oil Propanetriyl-1,2,3-triyl tris (decanoate) 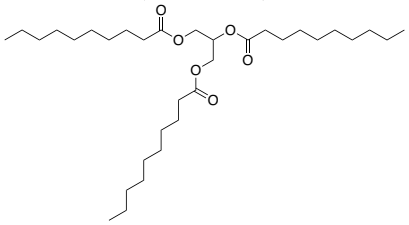 Glycerol tricaprylate 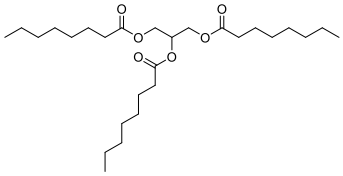 Dinonanoin monocaprylin 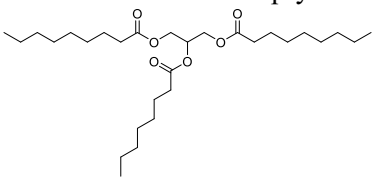	n-Octanoic acid isopropryl ester 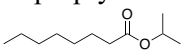 Methyl ester decanoic acid 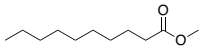 i-Propyl decanoate 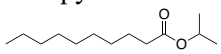	Formaldehyde  Acetaldehyde  Acetone  Propionaldehyde  1,3-Dihyroxypropanone 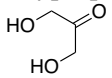 2-Butanone  n-Butanal 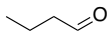 2-Pentanone 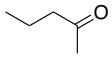 n-Pentanal 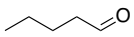 n-Hexanal 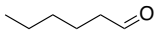 2-Hexanone 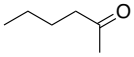 2-Heptanone 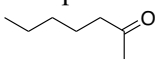 n-Heptanal 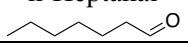	n-Tridecan-1-ol 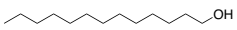

Table S5. Identified vaping emission products from SQL using GC/EI-MS analysis

Liquid Diluent	Alkanes	Carbonyls
Squalane 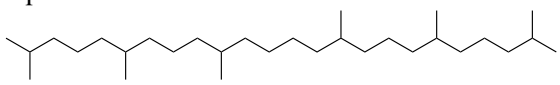	4-ethyl-octane 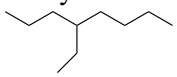	Acetaldehyde 
	2,6,10-Trimethyl-dodecane 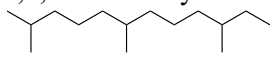	Acetone 
	2,6,10-Trimethyl-tetradecane 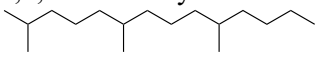	n-Pentanal 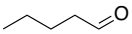
	2,6,10-Tetramethyl hexadecane 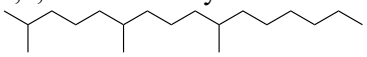	2-Octanone 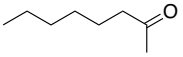
	2,6,10,15-tetramethyl heptadecane 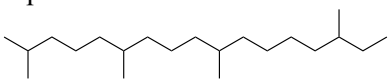	3-Methylpentanal 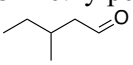
		n-Nonanal 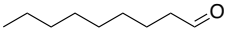
		5-Methoxy-2-pentanone 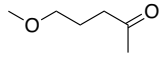
	Products with hydroxyl groups	
	6,10,14-Trimethyl-pentadecan-2-ol 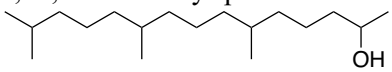	

Table S6. Identified vaping emission products from VE using GC/EI-MS analysis

Liquid Diluent	Carbonyls	Products with hydroxyl groups
Vitamin E 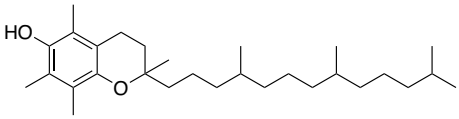	Acetone 	3,7,11-Trimethyl-1-dodecanol 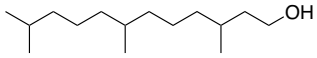
	Quinone-like products	
	Duroquinone 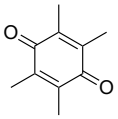	

Table S7. Identified vaping emission products from VEA using GC/EI-MS analysis

Liquid Diluent	Carbonyls	Products with hydroxyl groups
Vitamin E acetate 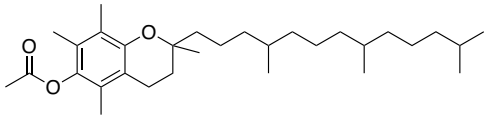	Acetone 	Vitamin E 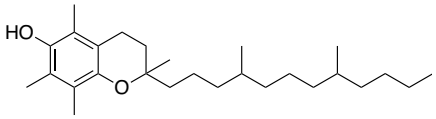
		3,7,11-Trimethyl-1-dodecanol 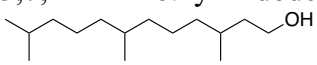
	Quinone-like products	
	Duroquinone 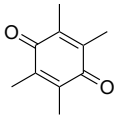	Durohydroquinone 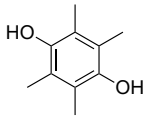

Table S8. Identified vaping emission products from TEC using GC/EI-MS analysis

Liquid Diluent	Esters
Triethyl citrate 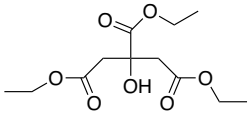	Diethyl ester Propanedioic acid 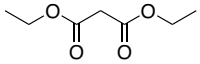 Malonic acid diisopropyl ester 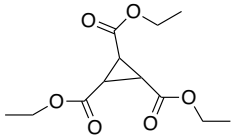 Diethyl ester Propanedioic acid 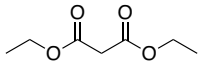 o-Acetylcitric acid triethyl ester 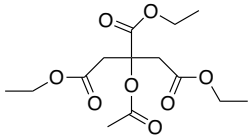

Table S9. Identified vaping products (with relative abundance larger than 5%) from PG ($C_3H_8O_2$) using ESI-Q-TOF-MS analysis

Unvaped PG						Vaped PG					
Proposed formula	Ion	Measured m/z	Theoretical m/z	Diff (mDa)	DBE	Proposed formula	Ion	Measured m/z	Theoretical m/z	Diff (mDa)	DBE
$C_6H_{14}O_3$	(M+Na)+	157.0838	157.0835	-0.29	0	$C_6H_{14}O_3$	(M+Na)+	157.0836	157.0835	-0.12	0
$C_9H_6O_3$	(M+H)+	163.038	163.039	0.93	7	$C_{23}H_{16}O_3$	(M+H)+	341.118	341.1172	-0.74	16
$C_6H_{10}O_5$	(M+H)+	163.0601	163.0601	-0.03	2	$C_{17}H_{26}O_{10}$	(M+Na)+	413.1404	413.1418	1.38	5
$C_8H_{18}O_5$	(M+Na)+	217.1042	217.1046	0.44	0						
$C_{12}H_{14}O_4$	(M+Na)+	245.0771	245.0784	1.28	6						
$C_{10}H_{18}O_{11}$	(M+Na)+	337.0741	337.0741	0.05	2						
$C_{16}H_{18}O_{10}$	(M+H)+	372.0998	372.1007	0.89	8						
$C_{18}H_{18}O_{11}$	(M+H)+	411.0921	411.0922	0.06	10						
$C_{12}H_{22}O_{14}$	(M+Na)+	413.0902	413.0902	-0.02	2						
$C_{30}H_{14}O_2$	(M+Na)+	429.089	429.0886	-0.35	24						
$C_{31}H_{28}O_8$	(M+H)+	529.1854	529.1857	0.26	18						
$C_{19}H_{28}O_{19}$	(M+H)+	561.1287	561.1298	1.10	6						
$C_{41}H_{24}O_6$	(M+Na)+	635.1462	635.1465	0.32	30						
$C_{22}H_{38}O_{24}$	(M+Na)+	709.1653	709.1645	-0.80	4						
$C_{55}H_{26}O_6$	(M+H)+	784.1824	784.1836	1.17	43						
$C_{54}H_{32}O_{11}$	(M+H)+	857.203	857.2017	-1.24	39						
$C_{35}H_{46}O_{29}$	(M+H)+	931.2207	931.2198	-0.99	13						

Table S10. Identified vaping products (with relative abundance larger than 5%) from VG using ESI-Q-TOF-MS analysis

Unvaped VG						Vaped VG					
Proposed formula	Ion	Measured m/z	Theoretical m/z	Diff (mDa)	DBE	Proposed formula	Ion	Measured m/z	Theoretical m/z	Diff (mDa)	DBE
$C_6H_{12}O_4$	(M+Na)+	171.0615	171.0628	1.32	1	$C_6H_{12}O_4$	(M+Na)+	171.0618	171.0628	1.00	1
						$C_{14}H_6O_5$	(M+H)+	135.0295	135.0288	-0.70	2
						$C_5H_2O_{10}$	(M+H)+	222.9713	222.9721	0.79	5
						$C_{13}H_{10}O_3$	(M+Na)+	237.0516	237.0522	0.66	9
						$C_{23}H_{28}O_{12}$	(M+H)+	497.1648	497.1654	0.56	10
						$C_{33}H_{32}O_9$	(M+Na)+	595.194	595.1939	-0.17	18
						$C_{40}H_4O_7$	(M+H)+	597.0022	597.0030	0.82	39
						$C_{30}H_{32}O_{13}$	(M+Na)+	623.1740	623.1735	-0.49	15
						$C_{40}H_{78}O_3$	(M+Na)+	629.5833	629.5843	1.03	2
						$C_{39}H_{54}O_9$	(M+H)+	667.3857	667.3841	-1.65	13
						$C_{36}H_{36}O_{14}$	(M+H)+	693.2177	693.2178	0.04	19
						$C_{50}H_{34}O_5$	(M+Na)+	737.2296	737.2298	0.24	34
						$C_{60}H_{96}O_8$	(M+Na)+	967.6983	967.6997	1.48	13

Table S11. Identified vaping products (with relative abundance larger than 5%) from MCT using ESI-Q-TOF-MS analysis

Unvaped MCT						Vaped MCT					
Proposed formula	Ion	Measured m/z	Theoretical m/z	Diff (mDa)	DBE	Proposed formula	Ion	Measured m/z	Theoretical m/z	Diff (mDa)	DBE
$C_{19}H_{34}O_4$	(M+H)+	327.2529	327.2530	0.13	3	$C_{19}H_{34}O_4$	(M+H)+	327.2528	327.2530	0.14	3
$C_{27}H_{50}O_6$	(M+Na)+	494.3535	494.3534	-0.11	3	$C_{27}H_{50}O_6$	(M+Na)+	494.3536	494.3534	-0.21	3
$C_{29}H_{54}O_6$	(M+Na)+	522.3853	522.3847	-0.63	3	$C_{29}H_{54}O_6$	(M+Na)+	522.3853	522.3847	-0.62	3
$C_{31}H_{58}O_6$	(M+Na)+	550.4164	550.4160	-0.46	3						

Table S12. Identified vaping products (with abundance larger than 5%) from SQL using ESI-Q-TOF-MS analysis

Unvaped SQL						Vaped SQL					
Proposed formula	Ion	Measured m/z	Theoretical m/z	Diff (mDa)	DBE	Proposed formula	Ion	Measured m/z	Theoretical m/z	Diff (mDa)	DBE
						$C_{19}H_{36}O_2$	(M+H)+	297.2769	297.2788	1.95	2
							(M+Na)+	319.2603	319.2068	0.46	2
						$C_{19}H_{34}O_3$	(M+Na)+	333.2382	333.2400	1.81	3
						$C_{19}H_{36}O_3$	(M+Na)+	335.2550	335.2557	0.67	2
						$C_{21}H_{40}O_3$	(M+Na)+	363.2877	363.2870	-0.72	2
						$C_{22}H_{40}O_3$	(M+Na)+	375.2873	375.2870	-0.35	3
						$C_{22}H_{42}O_2$	(M+H)+	339.3241	339.3258	1.61	2
						$C_{22}H_{44}O_3$	(M+Na)+	379.3176	379.3183	0.67	1
						$C_{22}H_{46}O_2$	(M+Na)+	365.3388	365.3390	0.21	0
						$C_{24}H_{40}O_3$	(M+H)+	377.3048	377.3050	0.21	5
						$C_{24}H_{46}O_2$	(M+H)+	367.3555	367.3571	1.53	2
							(M+Na)+	390.3423	290.3424	0.11	2
						$C_{24}H_{44}O$	(M+H)+	349.3477	349.3465	-1.17	3
						$C_{27}H_{52}O_2$	(M+H)+	409.4041	409.4040	-0.13	2
							(M+Na)+	431.3855	431.3860	0.50	2
						$C_{24}H_{44}O_3$	(M+Na)+	403.3166	403.3188	1.68	3
						$C_{24}H_{46}O$	(M+H)+	351.3621	351.3621	0	2
						$C_{27}H_{52}O_2$	(M+Na)+	391.3537	391.3547	0.92	1
						$C_{25}H_{48}O_2$	(M+H)+	381.3708	381.3727	1.95	2
						$C_{25}H_{50}O_2$	(M+Na)+	405.3689	405.3703	1.42	1
						$C_{25}H_{52}O_2$	(M+Na)+	407.3851	407.2860	0.88	0
						$C_{26}H_{50}O_3$	(M+Na)+	433.3633	433.3652	1.88	2
						$C_{27}H_{52}O_3$	(M+Na)+	447.3798	447.3809	1.12	2
						$C_{27}H_{54}O_2$	(M+Na)+	433.4008	433.4016	0.79	1
						$C_{27}H_{54}O_3$	(M+Na)+	449.3955	449.3965	1.03	1
						$C_{28}H_{52}O$	(M+Na)+	427.3921	427.3910	-1.08	3
						$C_{28}H_{56}O$	(M+Na)+	431.4232	431.4223	-0.86	1
						$C_{28}H_{56}O_3$	(M+Na)+	463.4117	463.4122	0.45	1
						$C_{28}H_{58}$	(M+Na)+	417.4422	417.4431	0.87	0
						$C_{28}H_{58}O$	(M+Na)+	433.4391	433.4380	-1.11	0
						$C_{28}H_{58}O_2$	(M+Na)+	449.4333	449.4329	-0.4	0
						$C_{28}H_{58}O_3$	(M+Na)+	465.4279	465.4278	-0.07	0
						$C_{29}H_{54}O_3$	(M+Na)+	473.3969	473.3965	-0.39	3
						$C_{29}H_{56}O$	(M+H)+	421.4390	421.4404	1.37	2
						$C_{29}H_{56}O_2$	(M+Na)+	459.4155	459.4173	1.73	2

	$C_{30}H_{52}O$	(M+H)+	429.4099	429.4091	-0.85	5
	$C_{30}H_{52}O_2$	(M+Na)+	467.3839	467.3860	2.00	5
	$C_{30}H_{56}O_2$	(M+Na)+	472.4189	472.4207	1.77	3
	$C_{30}H_{58}O$	(M+H)+	436.4585	436.4595	0.99	2
	$C_{30}H_{54}O_2$	(M+H)+	447.4186	447.4197	1.06	4
		(M+Na)+	469.3999	469.4016	1.72	4
	$C_{30}H_{58}O_2$	(M+H)+	451.4497	451.4510	1.24	2
	$C_{30}H_{58}O_3$	(M+H)+	467.4442	467.4459	1.72	2
	$C_{30}H_{60}O_2$	(M+Na)+	476.4502	476.4520	1.78	1
	$C_{30}H_{60}O_3$	(M+Na)+	492.4456	492.4469	1.32	1

Table S13. Identified vaping products (with relative abundance larger than 5%) from VE using ESI-Q-TOF-MS analysis

Unvaped VE						Vaped VE					
Proposed formula	Ion	Measured m/z	Theoretical m/z	Diff (mDa)	DBE	Proposed formula	Ion	Measured m/z	Theoretical m/z	Diff (mDa)	DBE
$C_{29}H_{48}O_2$	(M+H)+	429.3723	429.3727	0.45	6	$C_6H_{12}O$	(M+H)+	101.0955	101.0961	0.55	1
$C_{29}H_{50}O_2$	(M+H)+	430.3803	430.3811	-0.80	5	$C_{29}H_{50}O_2$	(M+H)+	430.3801	430.3811	-0.93	5
$C_{27}H_{50}O_3$	(M+Na)+	446.3700	446.3686	-1.39	3	$C_{27}H_{50}O_3$	(M+Na)+	446.3700	446.3686	-1.40	3
						$C_{29}H_{50}O_4$	(M+Na)+	485.3590	485.3601	1.11	5

Table S14. Identified vaping products (with relative abundance larger than 5%) from VEA using ESI-Q-TOF-MS analysis

Unvaped VEA						Vaped VEA					
Proposed formula	Ion	Measured m/z	Theoretical m/z	Diff (mDa)	DBE	Proposed formula	Ion	Measured m/z	Theoretical m/z	Diff (mDa)	DBE
$C_{31}H_{52}O_3$	(M+H)+	474.4027	474.4023	-0.41	6	$C_{31}H_{52}O_3$	(M+H)+	474.4028	474.4023	-0.48	6
	(M+Na)+	496.3847	496.3843	-0.46	6		(M+Na)+	496.3848	496.3843	-0.57	6

Table S15. Identified vaping products (with relative abundance larger than 5%) from TEC using ESI-Q-TOF-MS analysis

Unvaped TEC						Vaped TEC					
Proposed formula	Ion	Measured m/z	Theoretical m/z	Diff (mDa)	DBE	Proposed formula	Ion	Measured m/z	Theoretical m/z	Diff (mDa)	DBE
$C_7H_8O_4$	(M+H)+	157.0496	157.0495	-0.09	4	$C_7H_8O_4$	(M+H)+	157.0496	157.0495	-0.09	4
$C_{12}H_{20}O_7$	(M+Na)+	300.1132	300.1135	0.38	3	$C_{12}H_{20}O_7$	(M+Na)+	300.1132	300.1135	0.38	3
$C_{24}H_{40}O_{14}$	(M+Na)+	575.2316	575.2310	-0.61	5	$C_{24}H_{40}O_{14}$	(M+Na)+	575.2316	575.2310	-0.61	5

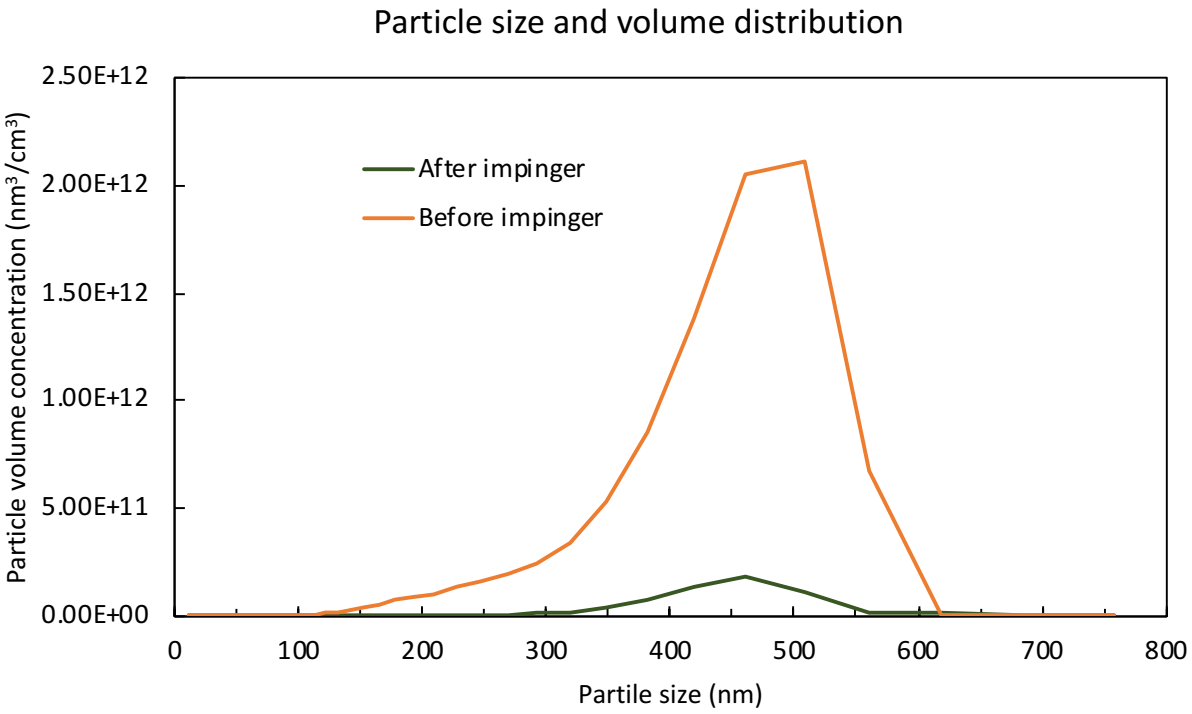

Figure S1. The particle size and volume distribution in the mainstream before and after the tandem impinger collection. Note that only 1 puff was collected when connecting a scanning electron mobility spectrometer (SEMS, Brechtel Manufacturing Inc.) to the inflow vaping plume, while a puffing patter of 4s e-cigarette on and 30 s rest time (1 puff cycle = 35 s) was applied when connecting SEMS to the outflow of the impinger collection. The particle volume concentration of 1 puff in one SEMS sampling cycle (3 min) was 9.09×10^{12} nm^3/cm^3. The particle volume concentration outflow of impinger was 3.77×10^{9} nm^3/cm^3. Assuming the aerosol collection efficiency was η, then $\eta+ \eta(1-\eta) = 1- 3.77\times10^{11}/9.09\times10^{12}=0.96$ and $\eta = 80\%$.

(A) Duroquinone

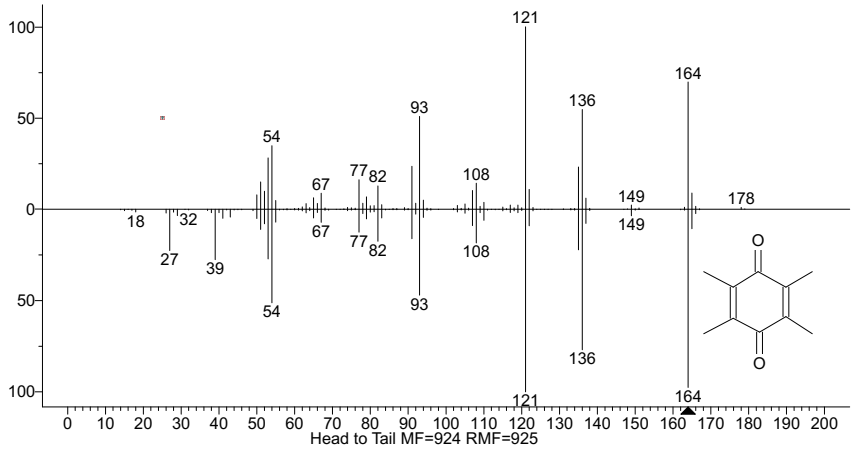

(B) Durohydroquinone

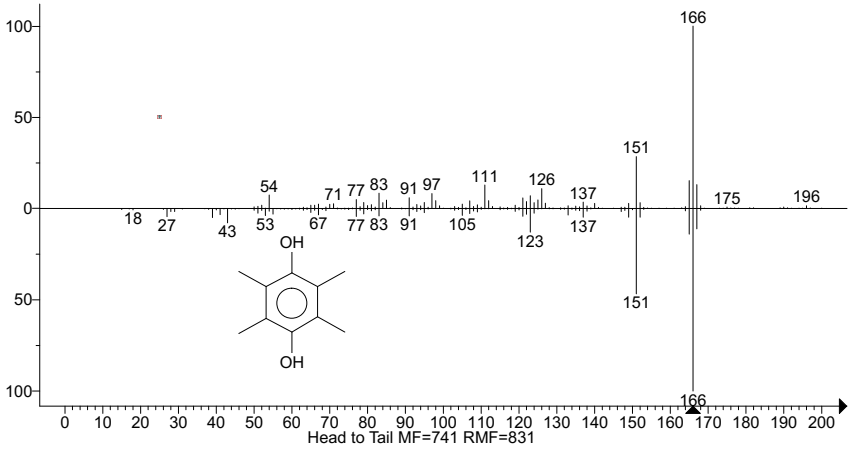

Figure S2. The experimental and NIST library spectrum of (A) duroquinone (match rate = 84.0%) and durohydroquinone (match rate = 49.9%).

Reference

(1) Jiang, H., Frie, A. L., Lavi, A., Chen, J. Y., Zhang, H., Bahreini, R., and Lin, Y.-H. (2019) Brown carbon formation from nighttime chemistry of unsaturated heterocyclic volatile organic compounds. *Environ. Sci. Technol. Lett. 6*, 184-190.

(2) Yu, J., Jeffries, H. E., and Le Lacheur, R. M. (1995) Identifying airborne carbonyl compounds in isoprene atmospheric photooxidation products by their pfbha oximes using gas chromatography/ion trap mass spectrometry. *Environ. Sci. Technol. 29*, 1923-1932.

(3) Chen, J. Y., Jiang, H., Chen, S. J., Cullen, C., Ahmed, C. M. S., and Lin, Y.-H. (2019) Characterization of electrophilicity and oxidative potential of atmospheric carbonyls. *Environ. Sci. Processes Impacts 21*, 856-866.

(4) Reddel, R. R., Ke, Y., Gerwin, B. I., McMenamin, M. G., Lechner, J. F., Su, R. T., Brash, D. E., Park, J.-B., Rhim, J. S., and Harris, C. C. (1988) Transformation of human bronchial epithelial cells by infection with sv40 or adenovirus-12 sv40 hybrid virus, or transfection via strontium phosphate coprecipitation with a plasmid containing sv40 early region genes. *Cancer Res. 48*, 1904-1909.